TECHNISCHE MECHANIK
European Journal of Engineering Mechanics
Diamond Open Access
journal homepage: www.ovgu.de/techmech

Tech. Mech., Vol. 46, Is. 1, (2026), 104–114
Received: 17.11.2025
Accepted: 31.01.2026
Available online: 16.02.2026

Numerical Study of Liquid Embolization in Intravascular Treatment Using a Moving Particle Semi-implicit Method

Takuya Natsume[1], Marie Oshima[2]*, and Nobuhiko Mukai[3]

[1] Graduate School of Integrative Science and Engineering, Tokyo City University, Japan
[2] Interfaculty Initiative in Information Studies; Institute of Industrial Science, the University of Tokyo, Japan
[3] Faculty of Informatics, Tokyo University of Information Sciences

Abstract: Subarachnoid hemorrhage is caused mainly by cerebral aneurysm rupture. Since subarachnoid hemorrhage has not only high mortality but also high possibility for complications, it is important to prevent aneurysm rupturing by performing an intravascular treatment.
The advantage of the recently developed photocurable liquid embolization is its controllability compared to conventional treatment such as coiling or clipping. However, as the treatment has not been evaluated extensively, this study presents a numerical method to investigate applicability of intravascular treatment using photocurable liquid embolization. The process of photocurable liquid embolization is complicated and involves both geometrical and topological changes like separation. Therefore, a particle method, particularly the moving particle semi-implicit method was used in this paper. In order to replicate the treatment, which involves injecting embolization liquid into blood in the aneurysm, the interfacial tension requires two types of interactions :1) the one between blood (water) and embolization liquid (viscous fluid) and 2) the other between embolization liquid (viscous fluid) and catheter (cylindrical Teflon tube) with wettability. We developed an efficient numerical method that considers the effects of highly viscous fluids of liquid embolization and wettability of a catheter. The proposed method was applied to a simplified problem by injecting highly viscous fluid to water to replicate the intravascular treatment. The simulation results were compared to experimental data and showed good agreement with the experiments.

Keywords: Moving particle semi-implicit method, highly viscous fluid, wettability, photocurable liquid embolization, cerebral aneurysm

1 Introduction

Subarachnoid hemorrhage is a serious cerebral disorder. Due to high mortality rate and severe subsequent complications after the incidence of subarachnoid hemorrhage, a patient at high risk is often recommended surgery (Yamada et al. (2003)). Since subarachnoid hemorrhage generally occurs in patients with a relatively large cerebral aneurysm, surgery is necessary to prevent the aneurysm rupture. There are mainly two types of conventional surgical treatments: coiling and clipping. Coiling is less invasive than clipping and therefore more widely used. However, it is an expensive procedure that requires a large number of expensive coils. In addition, once inserted into the aneurysm, the coils cannot be retracted. In view of the limitations of coiling, liquid embolization methods like Onxy have gained attention (Molyneux et al. (2004)). In particular, photocurable liquid embolization has been developed as a novel treatment. The advantage of photocurable liquid embolization is its controllability compared to the conventional treatments.
Photocurable liquid embolization is still under development for a clinical application. A numerical simulation is a valuable technique to elucidate the mechanism as well as to examine the procedure. However, replicating the flow behavior of photocurable liquid embolization by simulation is quite challenging. Since it is injected into aneurysm from catheter, its process is quite complicated and involves geometrical and topological changes like separation. Therefore, the simulation is required to perform not only flow analysis but also analyze interaction between blood flow and liquid for embolization and that between liquid for embolization and catheter with consideration of wettability.
To solve these complex issues, liquid embolization process was simplified. Specifically, to capture essential physics, viscous fluid imitating embolization liquid was injected into water instead of blood through a Teflon tube assumed to be a catheter. Since the embolization happened through topological changes, the moving particle semi-implicit (MPS) method was used in this study (Koshizuka and Oka (1996)). A stabilization method was investigated to reduce numerical instability caused by pressure oscillations (Tanaka and Masunaga (2010); Irebe and Nakazawa (2011); Monaghan (2000)). In addition, we developed an efficient numerical method that considers the interfacial tension between water and highly viscous fluids of liquid embolization as well as the interfacial tension with the wettability of the viscous fluid on the catheter. There are some interfacial models such as CFS model developed by Nomura et al. (2001), which considers a volume force. In this paper, the interfacial model with wettability plays an important role, so that we need to consider the wettability not only in the interface between embolization liquid and catheter but also in the interface between blood, embolization, and catheter. In general, the contact angle is needed in the simulation. However,

* E-mail address: marie@iis.u-tokyo.ac.jp
doi: 10.24352/UB.OVGU-2026-011

it is quite difficult to obtain the contact angle in the interface between blood, embolization liquid, and catheter. Therefore, a new interfacial model with the wettability was developed using the potential model developed by Kondo et al. (2007), which formalizes an intermolecular force. However, these models are designed for force in single phase flow, and not for liquid-liquid two phase flow as in the present study. To consider the influence of interaction between two-phase flows with the contact on the wall in the interfacial boundary, this study developed a method based on the potential model developed by Kondo et al. (2007) and Mukai et al. (2024) combining it with the interfacial tension model developed by Ishii and Sugii (2012).
Therefore, this paper aims to develop a new numerical technique based on the MPS method to simulate the injection of embolization liquid into aneurysm by considering the interaction between blood and liquid embolization and one between liquid embolization and catheter with wettability as well as one between blood, liquid embolization, and catheter with wettability. In order to validate the proposed method, the simulation results were compared to experimental data, in which the problem was simplified as a viscous fluid injected into water through a cylindrical Teflon tube (Natsume et al. (2021)). The simulations were performed using the same conditions used in the experiments. Even though the simulation results tended to have more elongated droplets compared to the droplets in the experiment, relatively good agreement between simulation and experiment was obtained.

2 Numerical Method

In this study, the MPS method was used to simulate the injection of a highly viscous fluid into water through a cylindrical Teflon tube, mimicking the injection of embolization liquid (highly viscous fluid) into blood (water) in an aneurysm through the catheter (cylindrical Teflon tube). Since this is a complex multi-physic problem, the simulation not only models the flow of water and highly viscous fluid but also the interaction between them. In addition, the present study developed the interfacial tension model to account for interactions between water and the viscous fluid as well as one between the viscous fluid and cylindrical tube, while considering wettability effects.

2.1 Governing Equations

The present method was applied to an injection problem involving a highly viscous fluid to replicate intravascular treatment. Therefore, flow simulations of incompressible Newtonian fluid are performed for water and viscous fluid. The governing equations consist of the continuity and Navier–Stokes equations as follows:

$$\frac{\partial u_i}{\partial x_i} = 0 \tag{1}$$

$$\frac{\partial u_i}{\partial t} + u_j \frac{\partial u_i}{\partial x_j} = -\frac{1}{\rho}\frac{\partial P}{\partial x_i} + \frac{\mu}{\rho}\frac{\partial^2 u_i}{\partial x_j^2} + F_i \tag{2}$$

where u is the velocity $[m/s]$, P is the pressure $[Pa]$, F is the external body force $[N]$, μ is the viscosity coefficient $[Pa \cdot s]$, ρ is the density $[kg/m^3]$, t is the time $[s]$, and x is the position in the Cartesian coordinate system $[m]$, respectively. The subscripts i and j represent x, y, and z corresponding to 1, 2, and 3.
The external body force F_i $[N]$ is given by

$$F_i = \rho g_i + F_i^{\text{inter}} \tag{3}$$

where g is the gravitational acceleration $[m/s^2]$, and F_i^{inter} is the interfacial tension $[N]$, respectively. The method to determine force F_i^{inter} is described in the later section.

2.2 MPS Method

The MPS method is based on particle interactions, discretizing the partial differential equation using a weight function to calculate an averaged interparticle distance. This study uses the weight function developed by Tamai and Koshizuka (2014), which is given by

$$w^{\overline{kl}} = \begin{cases} \left(\dfrac{r^{\overline{kl}}}{r_{\mathrm{e}}^k} - 1\right)^2, & \left(r^{\overline{kl}} \le r_{\mathrm{e}}^k\right) \\ 0, & \left(r_{\mathrm{e}}^k \le r^{\overline{kl}}\right) \end{cases} \tag{4}$$

where $r^{\overline{kl}}$ is the distance between particle k and l $[m]$, and the effective radius r_{e}^k is the radius of influence for the particle k $[m]$. The superscripts k and l represent the particle number while the superscript $\overline{kl}$ is used to describe a variable between the particle numbers k and l. In this study, r_{e}^k is set as 2.1 times the initial interparticle distance in the gradient and the divergence models while it is set as 3.1 times in the interfacial tension models.
The MPS method requires the density of particles, which is obtained by

$$n^k = \sum_{k \neq l} w^{\overline{kl}} \tag{5}$$

where n is the particle density $[m^{-3}]$, w is the weighted function, respectively.
The particle interaction model comprises the gradient, the divergence, and the Laplacian terms. The gradient term of particle k for an arbitrary scalar ϕ^k can be described in the following partial differential operators:

$$\frac{\partial \phi^k}{\partial x_i} = \left(M_{ij}^k\right)^{-1} b_j^k \tag{6}$$

$$M_{ij}^k = \frac{1}{n^0} \sum_{l \neq k} \frac{\left(r_i^l - r_i^k\right)\left(r_j^l - r_j^k\right)}{\left(r^{kl}\right)^2} w^{kl} \tag{7}$$

$$b_j^k = \frac{1}{n^0} \sum_{l \neq k} \frac{\phi^l - \hat{\phi}^k}{\left(r^{kl}\right)^2} \left(r_j^l - r_j^k\right) w^{kl} \tag{8}$$

where $n^o r$, and $\hat{\phi}$ are the particle density at the initial state $[m^{-3}]$, the coordinates of the particle $[m]$, and the smallest value of the scale ϕ within the effective radius, respectively.
The divergence of the velocity $\mathbf{u}$ is given by

$$\frac{\partial u_i^k}{\partial x_i} = \frac{d}{n^0} \sum_{l \neq k} \frac{\left(u_i^l - u_i^k\right) \cdot \left(r_i^l - r_i^k\right)}{\left(r^{\bar{kl}}\right)^2} w^{\bar{kl}} \tag{9}$$

where d is the dimension number.

$$\frac{\partial^2 \phi^k}{\partial x_j^2} = \frac{2d}{\lambda n^0} \sum_{l \neq k} (\phi^l - \phi^k) w^{\overline{kl}} \tag{10}$$

where λ is defined as

$$\lambda = \frac{\sum_{k \neq l} (r^{\overline{kl}})^2 w^{\overline{kl}}}{\sum_{k \neq l} w^{\overline{kl}}} \tag{11}$$

When the governing Eqs. (1) and (2) are solved, numerical instability may increase depending on the arrangement of particles. Therefore, the high-order MPS is used to avoid numerical instability. In general, the pressure Poisson equation is solved to obtain pressure. We applied the high-order method to the Laplacian term of pressure in the Poisson equations using the method based on Tanaka and Masunaga (2010); Irebe and Nakazawa (2011); Monaghan (2000). In addition, the high-order gradient model developed by Irebe and Nakazawa (2011) was applied to the pressure gradient term.

2.3 Interfacial Tension Model

The two types of interface force considered in this study are the one between blood (water) and liquid for embolization (viscous fluid) and the other between catheter (cylindrical Teflon tube) and liquid for embolization (viscous fluid). Therefore, when the interfacial tension F_i^{inter} is calculated, it is necessary to consider two types of the interfacial tension models: (1) the one between liquid and liquid and (2) the other between solid and liquid considering wettability.
In this study, the simulation is simplified as described in the previous section. Figure 1 describes the interfacial force between water and viscous fluid. A blue particle represents water, and a red represents viscous fluid.
Let us consider force balance in the region within the radius of influence $r_{\text{e}}^{k,\,\text{ave}}$ $[m]$ as shown in Fig. 1. The interfacial tension model in the present study is based on the potential model (Ishii and Sugii (2012)). The interfacial force between water and viscous fluid is given as follows:

$$\left(F^k\right)_i^{\text{in b-e}} = \frac{d\left(P^{\text{e}} - \overline{P^{\text{b}}}\right)}{h} n_i^{k-\text{in}} \tag{12}$$

where h is the thickness of the interface. The superscripts in, b, and e represent interface, blood, and embolization liquid. Therefore, $(F^k)_i^{\text{in b-e}}$ implies the interfacial force of the particle k between blood and embolization liquid $[N]$.

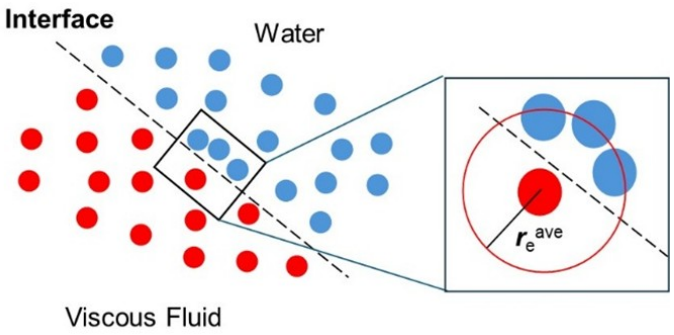

Fig. 1: Schematic illustration of the interfacial force between blood and liquid for embolization.

The pressure of blood is given by

$$P^{\mathrm{b}} = \frac{1}{\mathrm{N}} \sum_{l \neq k}^{\mathrm{N}} \overline{P^{\mathrm{b}}}\, w'^{\overline{kl}} \tag{13}$$

$$w'^{\overline{kl}} = \begin{cases} 1, & \left(r^{\overline{kl}} < r_{\mathrm{e}}^{\mathrm{ave}}\right), \\ 0, & \left(r_{\mathrm{e}}^{\mathrm{ave}} \leq r^{\overline{kl}}\right) \end{cases} \tag{14}$$

where N' and $w'^{\overline{kl}}$ are the number of blood particles within the radius of influence $r_{\mathrm{e}}^{\mathrm{ave}}$ and the weight function of blood particles within $r_{\mathrm{e}}^{\mathrm{ave}}$, respectively.
Since this study deals with the contact between a viscous fluid and cylindrical tube, it is important to include the effects of wettability. In general, the contact angle of the embolization liquid on the catheter is used to characterize wettability. However, it is difficult to obtain the angle. Therefore, this study developed a method to replicate the wettability by combining adhesion and spread of liquid on the solid surface of the catheter.
First, the particles at the interface between viscous fluid and cylindrical tube need to be distinguished. The following normal vector is used to identify the particles on such interface:

$$n_i^{k-\mathrm{in}} = \begin{cases} \dfrac{F_i^{k-1}}{\left|F_i^{k-1}\right|} & \left(\dfrac{\left|F_i^{k-1}\right|}{\left|F_i^{k-1}\right|^{\mathrm{flat}}} \geq \eta\right), \\ 0 & \left(\dfrac{\left|F_i^{k-1}\right|}{\left|F_i^{k-1}\right|^{\mathrm{flat}}} < \eta\right) \end{cases} \tag{15}$$

where n_i^{k-in} is the normal vector of the particle number k to the interfacial surface in the direction i. In this paper, η is set to be 0.2 (Ishii and Sugii (2012)).
Next, the identification of particles at the interfacial surface is performed to distinguish the particles, where wettability needs to be considered. Figures 2a and 2b show schematic illustrations of how particles are identified using the effective radius r_{e}^{st}. The blue particles in Fig 2a are reference particles. The grey particles in Figs. 2a and 2b represent the wall of cylindrical tube. The red particles in Fig. 2b are required to consider wettability between water, viscous fluid and tube wall while the black particles in Fig. 2b are required to consider wettability between viscous fluid and tube wall. In addition, the green ones in Fig. 2b are required to consider wettability between water and viscous fluid.
If the effects of adhesion in wettability are strong, the force balance can be expressed as follows:

$$F_i^{k-\mathrm{ad}} = F_i^{k-\mathrm{s}} + F_i^{k-\mathrm{l}} - F_i^{k-\mathrm{sl}} \tag{16}$$

where $F_i^{k-\mathrm{ad}}$ is the adhesion force of the particle k $[N]$, $F_i^{k-\mathrm{s}}$ is the force toward the cylinder wall of the particle k $[N]$, $F_i^{k-\mathrm{l}}$ is the force toward liquid of the particle k $[N]$, $F_i^{k-\mathrm{sl}}$ is the force between wall and liquid of the particle k $[N]$. The superscripts ad, s, l, and sl represent adhesion, solid, liquid, the interface between solid and liquid, respectively.
On the other hand, when the effects of spreading out are stronger, the force balance becomes

$$F_i^{k-\mathrm{sp}} = F_i^{k-\mathrm{s}} - F_i^{k-\mathrm{l}} - F_i^{k-\mathrm{sl}} \tag{17}$$

Where $F_i^{\mathrm{k-sp}}$ is the spreading force of the particle k, in which the superscript sp implies the effect of spreading.
Each term in Eqs. (16) and (17) can be obtained using the following potential model:

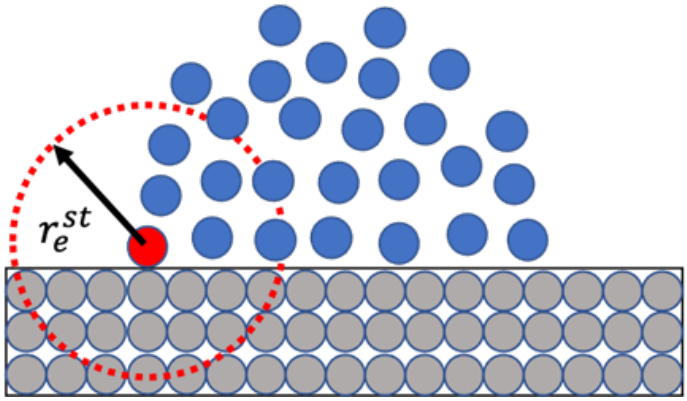

(a) Before identification

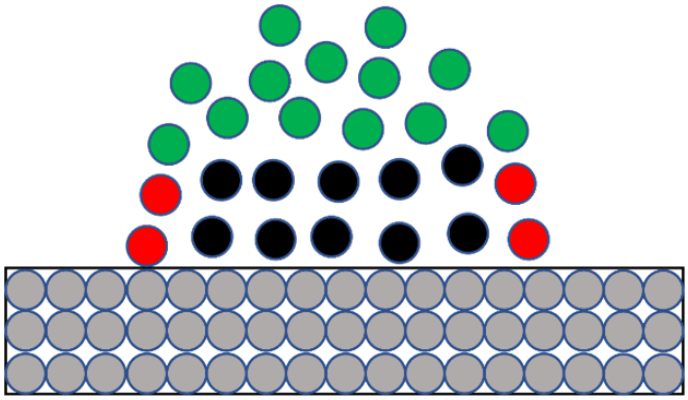

(b) After identification

Fig. 2: Schematic illustration of identification of particles subject to wettability.

$$F_i^{k-\alpha\alpha} = C^{\alpha\alpha} \sum_{l \neq k} f^{kl} \frac{r_i^l - r_i^k}{r^{\overline{kl}}} \tag{18}$$

The superscript $\alpha\alpha$ means l, s, or sl.
The interfacial potential between viscous fluid and cylindrical tube can be obtained by combining $F_i^{k-\mathrm{ad}}$ and $F_i^{k-\mathrm{sp}}$, which is given by

$$\left(F^k\right)_i^{\mathrm{in}\,l-\mathrm{w}} = F_i^{k-\mathrm{ad}} - H\,F_i^{k-\mathrm{sp}} \tag{19}$$

where H is the approximate Heaviside function given by

$$H = \begin{cases} 1, & x < -\dfrac{\Delta x}{2} \\ 1 - \dfrac{1}{2}\left(\dfrac{2x + \Delta x}{\Delta x} + \dfrac{1}{\pi}\sin\left(\dfrac{2\pi x}{\Delta x}\right)\right), & |x| \leq \dfrac{\Delta x}{2} \\ 0, & x > \dfrac{\Delta x}{2} \end{cases} \tag{20}$$

The domain and the range of the Heaviside function takes values in the range [0, 180] corresponding to the contact angle [0,1]. In order to define the simulation domain, generally, the contact angle is given in the simulation. However, in this study, the domain is defined by the potential force instead of the contact angle. Since the maximum value of the potential force became 75% of the basis one at the curvature 0, Δx became 0.75. Therefore, the domain of the Heaviside function was defined in the range [-0.375, +0.375]. The interfacial tension model in this paper, which comprises the interfacial tension model between liquid (blood) and liquid (embolization liquid) and the one between solid and liquid (blood or embolization liquid) considering wettability, can be defined as follows:

$$F_i^{k-\mathrm{inter}} = S^k \frac{d}{hA_0}\left[\left(\frac{1}{\frac{1}{\mathrm{N}}\sum_{l \neq k}\sin\phi^{\overline{kl}}}\right) - 1\right]\left(F^k\right)_{\mathrm{i}}^{\mathrm{in}\,l-\mathrm{w}} \tag{21}$$

where S^k is set as 1.0 for convex shape and -1.0 for concave shape. The superscripts inter and l-w represent the interface and interface between liquid (blood or embolization liquid) and catheter wall, respectively.

3 Results

The present method was applied to simulations of a droplet on various walls in order to validate the interfacial tension model with consideration of wettability. The droplet was placed on a wall with the contact angle $\theta = 90$ at an initial state as shown in Fig. 3a. The droplet changes its shape until it reaches the stable state. The contact angle θ [°] at the steady sate can be derived theoretically as follows:

$$\cos\vartheta = \frac{\gamma_s - \gamma_l}{\gamma_{sl}} \tag{22}$$

where γ is the interfacial tension force $[N]$ and the superscripts l, s, and sl means liquid, solid, and the interface between solid and liquid, respectively.
In this study, the simulations were performed to three different types of walls: glass, nylon, and adjusted wall. The adjusted wall was generated to obtain a certain contact angle by adjusting interfacial forces. The simulation results were compared to the theoretical values as summarized in Tab. 1.

Tab. 1: Contact angles for different wall materials

	Glass	**Nylon**	**Adjusted Wall**
Simulation	33°	69°	128°
Theory	30°	71°	130°

The simulation results are described in Figs. 3b–3d.

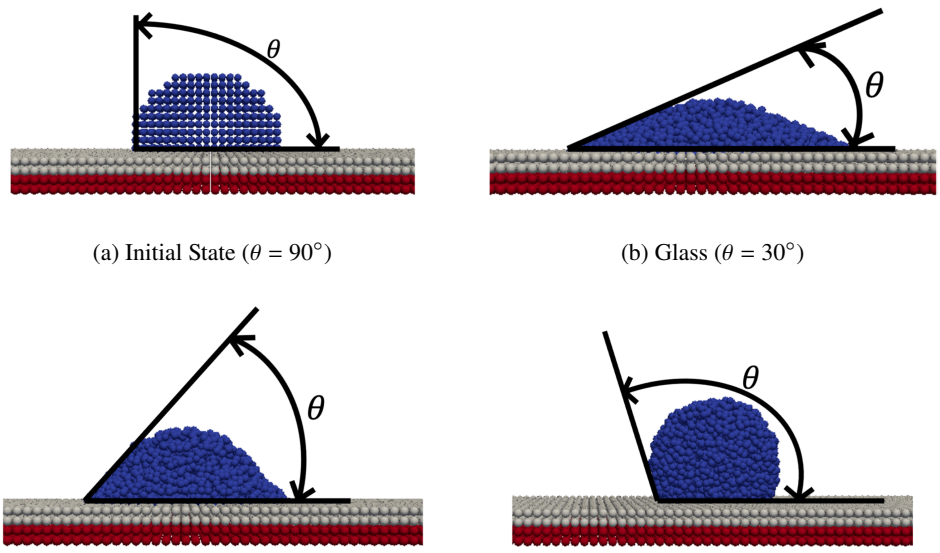

(a) Initial State ($\theta = 90°$)

(b) Glass ($\theta = 30°$)

(c) Nylon ($\theta = 71°$)

(d) Adjusted wall ($\theta = 130°$)

Fig. 3: Simulation results of the droplet on various walls

The errors between the simulation results and theoretical values are 10.0 % for the glass wall, 2.9 % for the nylon wall, and 1.5% for the adjusted wall with $\theta = 130°$. Therefore, the simulation results show good agreement with theoretical values.
The simulation results were compared to the experimental data to validate the present numerical method. The conditions for the experiment were applied for the numerical simulations. In this study, epoxy resin was used as embolization liquid and a Teflon tube was used as catheter in the experiment (Natsume et al. (2021)). Tab. 2 summarizes the experiment and simulation conditions. The particle size is 0.1 mm for the MPS simulation in this study. The experimental setup is shown in Fig. 4a. The simulation was performed using the analysis model as described in Fig. 4b under the same conditions as the experiment.
In order to examine the effects of wettability, a comparison was performed between simulation results obtained without and with considering wettability. Fig. 5a–5d present the results of comparison between without (images on the left) and with wettability (images on the right) at the different instantaneous times 1.0 s, 4.0 s, 7.0 s, and 10.0 s, respectively. If wettability is ignored, embolization liquid tends to be elongated due to gravitational force. On the other hand, if wettability is considered, embolization liquid tends to spread out at the edge of catheter against gravitational force, which makes embolization liquid less elongated. As time progresses, the upper part of the droplet is held in place by the catheter due to wettability, while gravity pulls the lower part of

Tab. 2: Experimental and simulation conditions

Physical Properties		**Value**
Density [kg/m^3]	Water	1.00×10^3
	Embolization Liquid	1.18×10^3
Dynamic viscosity [Pa·s]	Water	1.00×10^{-3}
	Embolization Liquid	7.42×10^{-3}
Inflow Velocity [m/s]		8.50×10^{-3}
Gravitational Acceleration [m/s^2]		9.8

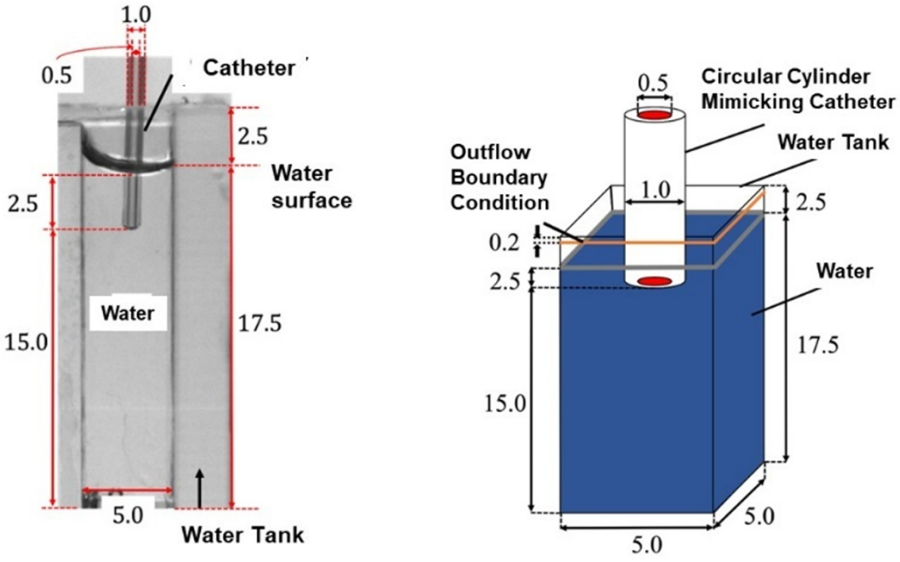

(a) Experimental model (b) Analysis model

Fig. 4: Experimental and analysis models.

the droplet, causing droplet constriction as shown in Figs 5b and 5c. Eventually, the droplet with wettability breaks up and is separated into two droplets while the one without wettability remains as one elongated droplet as shown in Fig. 5d.

Next, we compared the simulation results with experimental data. First, we compared the separation time, which is the time taken by a droplet to detach from the catheter, which is mimicked by the cylindrical Teflon tube. The experiment was performed six times while the simulation using the present method was performed three times. The average separation times for the experiments and simulation were 10.32 s and 7.09 s, respectively. The results of droplet volume for experiment and simulation were also compared. The average droplet volume was calculated over three trials for both the experimental measurements and simulations. The averaged droplet volume of simulation was 8.84×10^{-9} m^3 while it was 1.8×10^{-8} m^3 in the experiment. Both droplet volume and separation time were smaller than those in the experiments. Hence, separation in simulations tends to occur faster than that in experiments. This is caused by the underestimation of the interfacial tension compared to the gravitational force.

Let us compare the process of droplet formation at instantaneous times for both experiment and simulation. The images on the left in Figs. 6a–6d are the experimental measurement data while those on the right are the simulation results. Both experimental data and simulation results are compared at the same instantaneous times 1.00 s, 4.00 s, 7.00 s, and 10.00 s.

As illustrated in Figs 6, the droplet by the simulation tends to form faster than in the experiment, which leads to shorter droplet formation time and a smaller volume. Both the experiment and the simulation show that a droplet is forming at 1.03 s, while both droplets wet up along the catheter tip. The droplet has grown larger in both the experiment and the simulation at 4.0 s. However, the simulation exhibits more wetting along the catheter than the experiment. Furthermore, at 7.00 s, the droplet in the simulation elongates more in the vertical direction compared with the experimental droplet. By 10.00 s, the droplet in the experiment maintains a teardrop-like shape, whereas the droplet in the simulation is in a state just before detachment.

To examine the wetting behavior more closely, an enlarged view at 3.00 s is shown in Fig. 7.

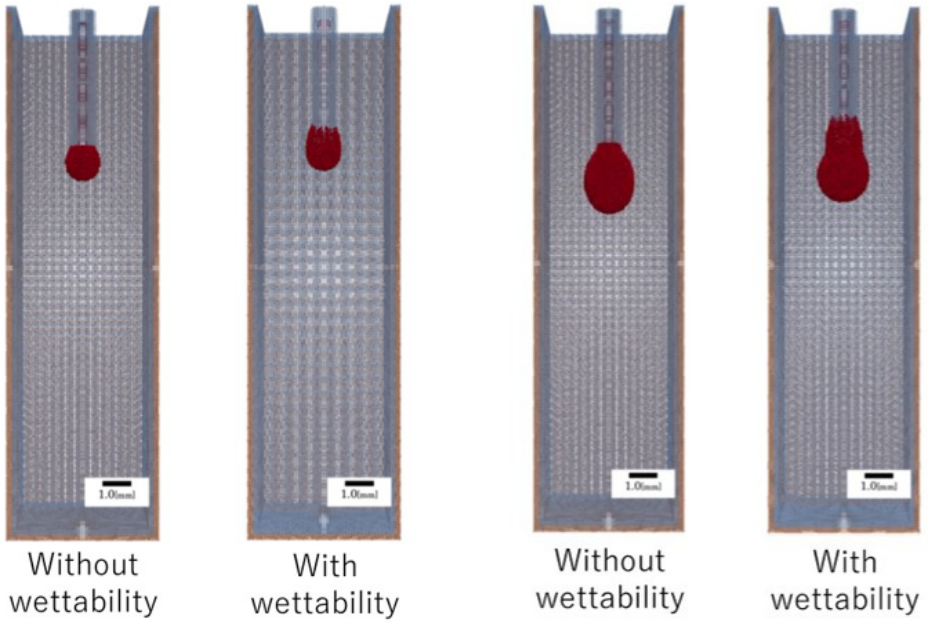

(a) Instantaneous time at 1.00 s (b) Instantaneous time at 4.00 s

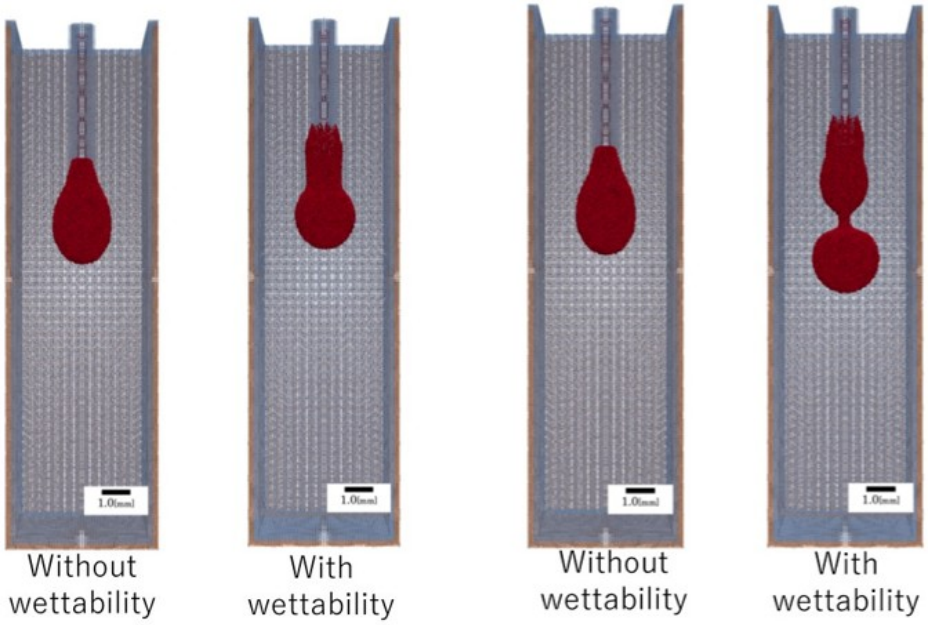

(c) Instantaneous time at 7.00 s (d) Instantaneous time at 10.00 s

Fig. 5: Comparison for investigation of wettability

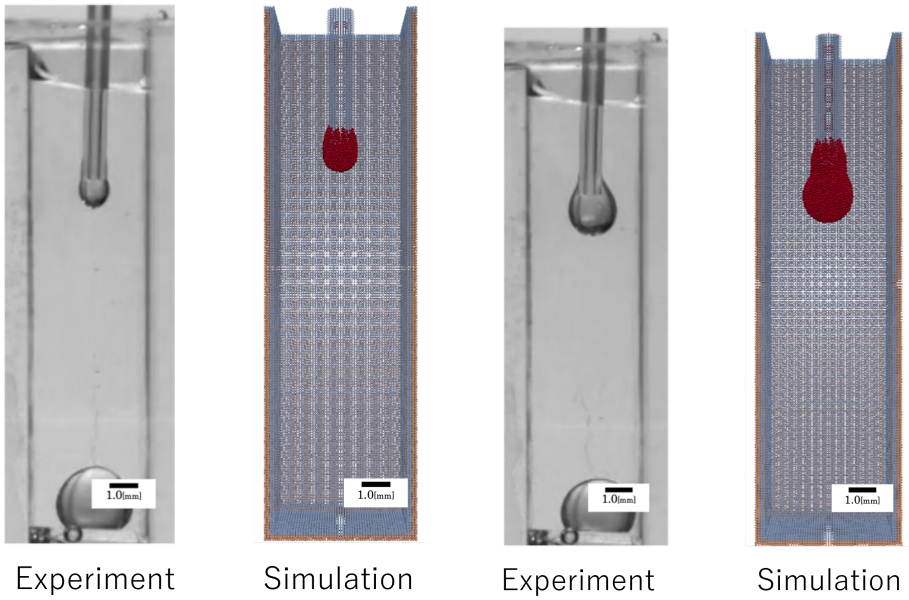

(a) Instantaneous time at 1.00 s (b) Instantaneous time at 4.00 s

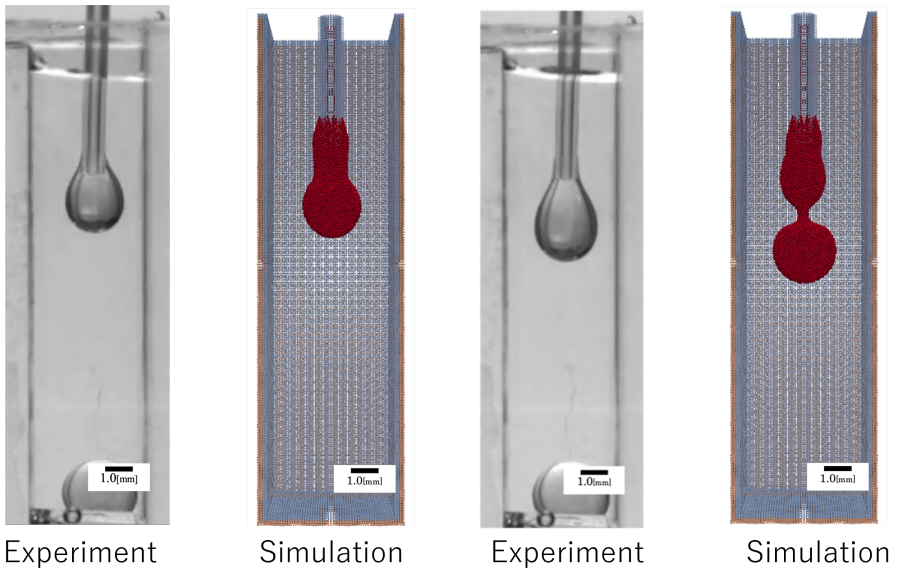

(c) Instantaneous time at 7.00 s (d) Instantaneous time at 10.00 s

Fig. 6: Comparison between experiment and simulation

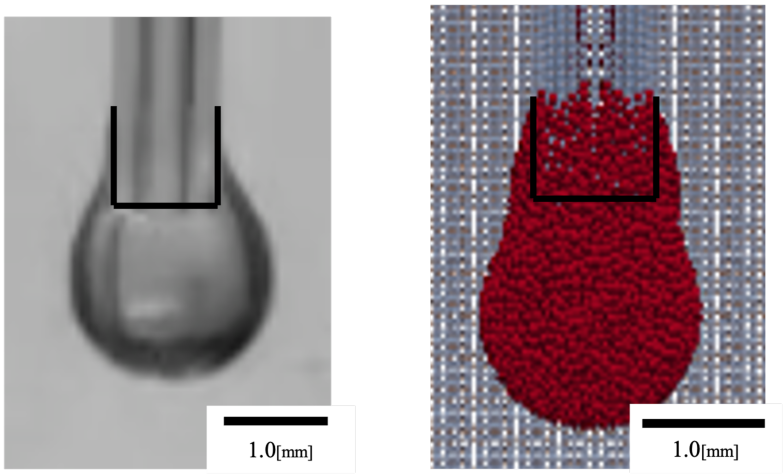

(a) Experiment (b) Simulation

Fig. 7: Enlarged images of both experiment and simulation near the catheter at 3.00 s

Since the catheter is hydrophilic, water (blood) tends to spread out along the catheter wall as shown in Fig. 7a. From Fig. 7b, it can be confirmed that the simulation exhibits greater wetting along the catheter. In addition, the droplet in the simulation is more elongated in the vertical direction due to consideration of wettability.

4 Conclusion

In order to investigate flow characteristics of photocurable liquid embolization as a novel treatment for cerebral aneurysms, a simulation method has been developed based on the MPS method to solve topological changes. In addition, the interfacial tension model was developed. Since the treatment involves injecting embolization liquid into blood in the aneurysm, the interfacial tension needs to consider two types of interactions: 1) the one between blood (water) and embolization liquid (viscous fluid) and 2) the other between embolization liquid (viscous fluid) and catheter (cylindrical Teflon tube) with wettability. The proposed interfacial tension model was incorporated into the MPS method and applied to the problem similar to the experimental setup, in which viscous fluid was injected into water through the cylindrical Teflon tube, which mimics the catheter. The experiment and simulation were conducted under the same conditions and compared. The simulation results showed relatively good agreement with those of the experiment. However, the simulation results showed a tendency to underestimate the interfacial force compared to the experimental results. Therefore, volume and separation time in the simulation were smaller than those in the experiment.

5 Acknowledgement

This research was supported by JSPS KAKENHI under Grant Number JP22H00190. The authors express appreciation to Dr. Masamichi Oishi for providing experimental data.

References

Y. Irebe and E. Nakazawa. Improvement of accuracy of a MPS method with a new gradient calculation model. *Journal of Japan Society of Civil Engineering*, 67:36–48, 2011. (in Japanese).

E. Ishii and T. Sugii. Development of surface tension model for a particle method. *Transactions of the Japan Society of Mechanical Engineers*, 78:1710–1725, 2012.

M. Kondo, S. Koshizuka, K. Suzuki, and M. Takimoto. Surface tension model using inter-particle force in particle method. In *Proceedings of the ASME/JSME 2007 5th Joint Fluids Engineering Conference*, volume 1, pages 93–98, San Diego, California, USA, 2007. ASME. doi: 10.1115/FEDSM2007-37215.

S. Koshizuka and Y. Oka. Moving-particle semi-implicit method for fragmentation of incompressible fluid. *Nuclear Science and Engineering*, 123(3):421–434, 1996.

A. J. Molyneux, S. Cekirge, I. Saatci, and G. Gál. Cerebral aneurysm multicenter European Onyx (CAMEO) trial: results of a prospective observational study in 20 European centers. *American Journal of Neuroradiology*, 25(1):39–51, 2004.

J. J. Monaghan. SPH without a tensile instability. *Journal of Computational Physics*, 159(2):290–311, 2000.

N. Mukai, T. Natsume, M. Oishi, and M. Oshima. Analysis of wettability using adhesion and spreading works. In *Proceedings of the 18th International Joint Conference on Computer Vision, Imaging and Computer Graphics Theory and Applications (VISIGRAPP 2024), Volume 1: GRAPP*, pages 230–236, 2024.

T. Natsume, M. Oishi, M. Oshima, and N. Mukai. Droplet formulation method for viscous fluid injection considering the effect of liquid-liquid two-phase flow. *ITE Transactions on Media Technology and Applications*, 9(1):33–41, 2021.

K. Nomura, S. Koshizuka, Y. Oka, and H. Obata. Numerical analysis of droplet breakup behavior using particle method. *Journal of Nuclear Science and Technology*, 38(12):1057–1064, 2001.

T. Tamai and S. Koshizuka. Least squares moving particle semi-implicit method: An arbitrary high order accurate meshfree Lagrangian approach for incompressible flow with free surfaces. *Computational Particle Mechanics*, 1(3):277–305, 2014.

M. Tanaka and T. Masunaga. Stabilization and smoothing of pressure in MPS method by quasi-compressibility. *Journal of Computational Physics*, 229(11):4279–4290, 2010.

S. Yamada, A. Koizumi, H. Iso, Y. Wada, Y. Watanabe, C. Date, A. Yamamoto, S. Kikuchi, Y. Inaba, H. Toyoshima, et al. Risk factors for fatal subarachnoid hemorrhage: the Japan Collaborative Cohort Study. *Stroke*, 34(12):2781–2787, 2003.